Potentiation of radiation sensitivity in breast tumor cells by the vitamin D$_3$ analogue, EB 1089, through promotion of autophagy and interference with proliferative recovery

Gerald DeMasters,[1] Xu Di,[1] Irene Newsham,[2] Robert Shiu,[3] and David A. Gewirtz[1]

[1]Departments of Pharmacology and Toxicology, Massey Cancer Center, Virginia Commonwealth University, Richmond, Virginia; [2]Brain Tumor Center, Department of Neuro-Oncology, The University of Texas M.D. Anderson Cancer Center, Houston, Texas; and [3]Department of Physiology, University of Manitoba, Winnipeg, Manitoba, Canada

Abstract

1,25-Dihydroxyvitamin D$_3$ and vitamin D$_3$ analogues, such as EB 1089, potentiate the response to ionizing radiation in breast tumor cells. The current studies address the basis for this interaction by evaluating DNA damage and repair, the effect of interference with reactive oxygen generation, the involvement of p53 and caspase-3, signaling through c-*myc*, as well as the induction of senescence and multiple modes of cell death. EB 1089 failed to increase the extent of radiation-induced DNA damage or to attenuate the rate of DNA repair. The reactive oxygen scavengers *N*-acetyl-L-cysteine and reduced glutathione failed to protect the cells from the promotion of cell death by EB 1089 and radiation. Whereas MCF-7 cells expressing caspase-3 showed significant apoptosis with radiation alone as well as with EB 1089 followed by radiation, EB 1089 maintained its ability to confer susceptibility to radiation-induced cell killing, in large part by interference with proliferative recovery. In contrast, in breast tumor cells lacking p53, where radiation promoted extensive apoptosis and the cells failed to recover after radiation treatment, EB 1089 failed to influence the effect of radiation. EB 1089 treatment interfered with radiation-induced suppression of c-*myc*; however, induction of c-*myc* did not prevent senescence by radiation alone or radiation-induced cell death promoted by EB 1089. EB 1089 did not increase the extent of micronucleation, indicative of mitotic catastrophe, induced by radiation alone. However, EB 1089 did promote extensive autophagic cell death in the irradiated cells. Taken together, these studies suggest that the effect of EB 1089 treatment on the radiation response is related in part to enhanced promotion of autophagic cell death and in part to interference with the proliferative recovery that occurs with radiation alone in p53 wild-type breast tumor cells. [Mol Cancer Ther 2006;5(11):2786–97]

Introduction

Apart from the established role of vitamin D$_3$ in the regulation of calcium homeostasis, numerous studies have shown the metabolically active form of vitamin D$_3$, 1,25-dihydroxyvitamin D$_3$ [1,25(OH)$_2$D$_3$], to have strong growth-inhibitory effects on a variety of tumor cell lines (1). Because hypercalcemia limits the concentrations of vitamin D$_3$ achievable in the clinic, several vitamin D$_3$ analogues, such as EB 1089 (seocalcitol), have been synthesized with reduced hypercalcemic activity. Although it is uncertain whether EB 1089 will itself be used in the clinic, the current studies examine this compound as a prototype of vitamin D$_3$ and vitamin D$_3$ analogues that could ultimately contribute to the effectiveness of conventional drug and radiation therapies.

Previous work from this laboratory has shown that vitamin D$_3$ [1,25(OH)$_2$D$_3$; cholecalciferol] and vitamin D$_3$ analogues, such as EB 1089 and ILX23-7553, enhance the response to both ionizing radiation (IR) and the antitumor drug, Adriamycin, in breast tumor cells (2–5); for IR, the effects of EB 1089 were also shown to occur in tumor cell xenografts (6). These findings are consistent with previous work by several research groups showing that vitamin D$_3$ and/or its analogues can potentiate the sensitivity to chemotherapeutic drugs in various experimental tumor systems (7–12).

Exposure of MCF-7 breast tumor cells to IR (either a single dose of 10 Gy or five fractionated doses of 2 Gy each) results in a prolonged state of growth arrest that has characteristics of premature or accelerated senescence (5, 13); this state of senescence arrest is followed by proliferative recovery in at least a subset of the cell population (5, 13). Exposure of the cells to EB 1089 before radiation promotes extensive cell death and markedly delays (but does not fully abrogate) the promotion of senescence, which is evident in residual surviving cells; furthermore, prior exposure to EB 1089 attenuates and delays the extent of proliferative recovery (5).

Multiple mechanisms have been shown to mediate the genomic, receptor-mediated based actions of vitamin D$_3$

doi:10.1158/1535-7163.MCT-06-0316

and its analogues in the tumor cell (1, 14). The current studies were done in an effort to identify the specific signaling pathways responsible for the observed interactions of vitamin D_3 and its analogues with radiation.

In view of the fact that EB 1089 converts a senescence response, which is essentially growth arrest, to one of cell death, the present studies were designed to focus on elements that are thought to be involved in the regulation of both growth arrest and cell death pathways. These include DNA damage and repair, the generation of reactive oxygen species (ROS), expression of the oncogene c-*myc*, and the tumor suppressor p53. In addition, this work was designed to address the multiple modes of cell death that could mediate the actions of EB 1089 in irradiated cells, specifically mitotic catastrophe and autophagy as well as apoptosis.

Materials and Methods

Materials

RPMI 1640 with L-glutamine, trypsin-EDTA (1×; 0.05% trypsin, 0.53 mmol/L EDTA-4 Na), penicillin/streptomycin (10,000 units/mL penicillin and 10 mg/mL streptomycin), and fetal bovine serum were obtained from Life Technologies (Gaithersburg, MD). Defined bovine calf serum was obtained from Hyclone Laboratories (Logan, UT). EB 1089 was provided by Dr. Lise Binderup of Leo Pharmaceuticals (Bellarup, Denmark). Reagents used for the terminal deoxynucleotidyl transferase–mediated dUTP nick end labeling assay (terminal transferase, reaction buffer, and fluorescein-dUTP) were purchased from Boehringer Mannheim (Indianapolis, IN). X-gal was obtained from Gold Biotechnology (St. Louis, MO). The following materials were obtained from Sigma Chemical (St. Louis, MO): trypan blue solution, formaldehyde, acetic acid, albumin bovine (bovine serum albumin), N-acetyl-L-cysteine, reduced glutathione (GSH), 4′,6-diamidino-2-phenylindole (DAPI), DMSO, propidium iodide, and bisbenzimide (Hoescht no. 33258). Acridine orange was purchased from Invitrogen (Eugene, OR). Z-VAD-fmk was purchased from Santa Cruz Biotechnology (Santa Cruz, CA).

Cell Lines

The p53 wild-type (WT) MCF-7 human breast tumor cell line was obtained from National Cancer Institute (Frederick, MD). MCF-7/E6 cells were a gift from Dr. Lynne Elmore of the Department of Pathology at Virginia Commonwealth University (Richmond, VA). MCF-7 cells engineered to express caspase-3 and MCF-7/35im cells with doxycycline-inducible myc have been described previously (refs. 13 and 15, respectively).

Cell Culture and Treatment

All cell lines were grown from frozen stocks in basal RPMI 1640 supplemented with 5% FCS, 5% bovine calf serum, 2 mmol/L L-glutamine, and penicillin/streptomycin (0.5 mL/100 mL medium) at 37°C under a humidified, 5% CO2 atmosphere. Cells were exposed to various doses of γ-IR using a ^{137}Ce irradiator. In the indicated studies, cells were exposed to 100 nmol/L EB 1089 for 72 hours before irradiation. This sequence of exposure was based on the studies by Wang et al. (16) and our own previous work (2–5), which have shown a requirement for prolonged incubation with vitamin D_3 or its analogues to promote sensitivity to Adriamycin and irradiation.

In the cases where the radiation doses were fractionated, five fractions of 2 Gy radiation were administered on three consecutive days (two fractions separated by 6 hours on the first 2 days followed by a fifth dose on the 3rd day). Cells were routinely subcultured by trypsinization (0.25% trypsin, 0.03% EDTA, Life Technologies) on reaching confluence. All experiments were done using cells during logarithmic growth and examined by microscope for bacterial or fungal contamination before experimental analysis. In addition, all cell lines were determined to be free of Mycoplasma.

Determination of Viable Cell Number

Cell viability was determined by trypan blue exclusion at various time points beginning 24 hours after the last dose of radiation. Cells were harvested by trypsinization, stained with 0.4% trypan blue dye, and counted using phase-contrast microscopy.

Terminal Deoxynucleotidyl Transferase – Mediated dUTP Nick End Labeling Assay for Apoptosis

The method of Gavrielli et al. (17) was used as an independent assessment of apoptotic cell death in combined cytospins containing both adherent and nonadherent cells. Cells were fixed and the fragmented DNA in cells undergoing apoptosis was detected using the *In situ* Cell Death Detection kit (Boehringer Mannheim), where strand breaks are end labeled with fluorescein-dUTP by the enzyme terminal transferase. Cells were then washed, mounted in Vectashield, and photographed using a Nikon (Melville, NY) fluorescent microscope.

Propidium Iodide Staining and Flow Cytometry

After treatment with EB 1089 and/or fractionated radiation, cells were harvested by trypsinization, pelleted by centrifugation, and washed twice with PBS. Cellular DNA was labeled by resuspending 1×10^6 cells in 1 mL propidium iodide staining solution (3.8 mmol/L sodium citrate, 0.05 mg/mL propidium iodide, 0.1% Triton X-100, and 9K units/mL RNase B). Cells were analyzed for DNA content with a Beckman Coulter (Fullerton, CA) XL-MCL flow cytometer. A minimum of 25,000 events was collected for each sample.

Alkaline Unwinding Assay

Bulk damage to DNA was assessed by alkaline unwinding following drug and radiation exposure as described in detail previously (3). Before radiation exposure, cells were harvested by trypsinization and washed in ice-cold PBS. Approximately 7×10^6 cells per condition were then resuspended in cold PBS and irradiated on ice. Cells were maintained on ice until assessment for DNA damage following the procedure described by Kantor and Schwartz (18). In studies assessing DNA repair, the cells were resuspended in fresh medium and irradiated at room temperature. The cells were then incubated at 37° C for 4 hours before evaluation of DNA damage.

β-Galactosidase Histochemical Staining

pH (6.0)-dependent β-galactosidase expression was used as a marker for senescence (19). At the appropriate times after treatment, cells were washed twice with PBS and fixed with 2% formaldehyde and 0.2% glutaradehyde for 5 minutes. The cells were then washed again with PBS and stained with a solution of 1 mg/mL 5-bromo-4-chloro-3-inolyl-β-galactosidase in dimethylformamide (20 mg/mL stock), 5 mmol/L potassium ferrocyanide, 5 mmol/L potassium ferricyanide, 150 mmol/L NaCl, 40 mmol/L citric acid/sodium phosphate (pH 6.0), and 2 mmol/L MgCl₂. Following overnight incubation at 37°C, the cells were washed twice with PBS and photographed with a light microscope.

Western Blot Analysis

After the indicated treatments, cells were washed in PBS and lysed using 100 to 200 μL lysis buffer containing protease inhibitors for 30 minutes on ice. Protein concentrations were determined by the Lowry method and equal aliquots of protein (10 or 20 μg) were separated using 15% SDS-PAGE. Proteins were transferred onto a nitrocellulose membrane and blocked in TBS-Tween 20 buffer containing 5% nonfat dry milk. Membranes were immunoblotted with respective antibodies and then incubated with horseradish peroxidase–conjugated secondary antibody. Proteins were visualized using an enhanced chemiluminescence kit from Pierce (Rockford, IL).

Detection of 53BP1 Foci by Immunohistochemistry

MCF-7 cells were seeded in eight-well chamber slides 24 hours before drug or radiation exposure (20). At the appropriate times after irradiation, cells were rinsed twice with PBS and then fixed with 3.7% paraformaldehyde in PBS for 10 minutes at room temperature. Cells were washed twice more with PBS and permeabilized in 0.5% NP40 in PBS for 10 minutes at room temperature. After two more washings with PBS, cells were blocked for 30 minutes in PBS with gelatin. The chamber slide basket was then removed before incubation with primary antibody.

53BP1 primary antibody was added onto cells, and slides were covered with parafilm. After overnight incubation at 4°C, slides were washed 3 × 5 minutes with PBS. The slides were then incubated with fluorescein-conjugated secondary antibody in PBS with gelatin for 1 hour. Following this 1 hour of incubation, slides were washed 3 × 5 minutes with PBS. Vectashield with DAPI was added to slides and coverslips were placed over cells. 53BP1 foci were visualized using an inverted fluorescent microscope. The average number of foci per cell was determined by dividing the total number of cells by the total number of foci for three representative fields per treatment condition.

Detection of Reactive Oxygen Generation

Dichlorofluorescein diacetate was used to detect ROS following exposure to EB 1089 and radiation (21). MCF-7 cells were seeded in T-25 flasks and treated as described in the cell viability study above. At the appropriate times after treatment, growth medium was removed and cells were incubated for 30 minutes with medium containing 5 μmol/L dichlorofluorescein diacetate. After 30 minutes, medium containing dichlorofluorescein diacetate was removed, and fresh medium was added to the flasks. Fluorescence was immediately visualized with an inverted fluorescent microscope.

Detection of Autophagic Cells by Staining with Acridine Orange

As a marker of autophagy, the volume of the cellular acidic compartment was visualized by acridine orange staining (22). Cells were seeded in T-25 flasks and treated as described above for the cell viability study. At the appropriate time points following treatment, cells were incubated with medium containing 1 μg/mL acridine orange (Molecular Probes, Eugene, OR) for 15 minutes. After 15 minutes, the acridine orange was removed and fluorescent micrographs were taken using an inverted fluorescent microscope. The number of cells with increased acidic vesicular organelles was determined by counting at least three representative fields per treatment condition.

Scoring of Micronuclei as an Indication of Mitotic Catastrophe

The induction of mitotic catastrophe was assessed by the formation of micronuclei (23). MCF-7 cells were seeded on glass coverslips and treated with EB 1089, 5 × 2 Gy IR, or EB 1089 followed by 5 × 2 Gy IR. At the appropriate times after irradiation, the cells on the coverslips were fixed with 3.7% paraformaldehyde in PBS for 10 minutes at room temperature. Cells were then fixed to glass slides using DAPI-containing Vectashield mounting medium. Pictures were taken using a Zeiss (Thornwood, NY) laser scanning microscope. Micronuclei were scored by first counting the percentage of binucleated cells. Micronuclei formation was then expressed as the fraction of binucleated cells that contained micronuclei.

Statistical Analysis

Statistical differences were determined using StatView statistical software. Comparisons were made using a one-way ANOVA followed by Fisher's protected least significance difference post-hoc test. Ps ≤ 0.05 were taken as statistically significant.

Results

Influence of EB 1089 on Radiation-Induced DNA Damage and DNA Repair

We have reported previously that EB 1089 fails to increase DNA damage induced by IR in MCF-7 cells (3). However, although no difference was evident in the extent of initial DNA damage by radiation alone and radiation preceded by EB 1089, the possibility remained that EB 1089 might influence the rate of DNA repair. Furthermore, the alkaline unwinding assay used to generate the previous data does not discriminate between single-strand breaks and double-strand breaks in DNA, where double-strand breaks are thought to be the lesion responsible for the cytotoxic effects of IR (24). We therefore examined whether the induction of DNA double-strand breaks by IR might be enhanced by EB 1089. Both alkaline unwinding (18) and 53BP1 foci formation (20) were used for assessment of DNA damage and repair.

Figure 1 shows the results of alkaline unwinding studies to assess the extent of bulk DNA damage and repair after radiation alone or EB 1089 followed by radiation. A single 10 Gy dose of radiation was used to increase the sensitivity of the assay, as the influence of EB 1089 on the radiation response is evident either with a single 10 Gy dose or with five fractionated doses of 2 Gy each (3, 5). The *F* value is an indicator of DNA damage, where an *F* value of 1 reflects intact (undamaged) DNA (18). Figure 1 indicates that the initial DNA damage induced by IR is not altered by prior exposure of the cells to EB 1089, consistent with our previous findings (3). In addition, the DNA damage is fully repaired within 4 hours with either radiation alone or with EB 1089 preceding the irradiation, indicating that EB 1089 does not influence the apparent rate or extent of DNA repair.

Figure 2 presents the results of studies assessing 53BP1 foci formation in MCF-7 cells exposed to either 2 Gy radiation alone or radiation preceded by treatment with 100 nmol/L EB 1089. A lower dose of radiation was used in these studies to allow for detection of a possible increase in damage with EB 1089. (In other studies, not shown, we have detected potentiation of the response to radiation by EB 1089 at a dose of 2 Gy). The initial induction of foci was assessed at 6 hours after irradiation. Figure 2A and B indicates that there was approximately one focus point in each control cell and that EB 1089 alone did not affect the number of foci formed. EB 1089 followed by radiation increased 53BP1 formation to an average of 4.5 foci per cell, a value that was not significantly different from that induced by radiation alone. These findings indicate that EB 1089 does not increase the extent of dsDNA damage induced by radiation, which is consistent with the data presented in Fig. 1.

To evaluate the effect of EB 1089 on repair of double-strand breaks in DNA, the decline in 53BP1 foci was monitored over a period of 48 hours. Figure 2A and B shows that the rate of decline in foci was essentially identical in cells treated with radiation alone and in cells exposed to EB 1089 before 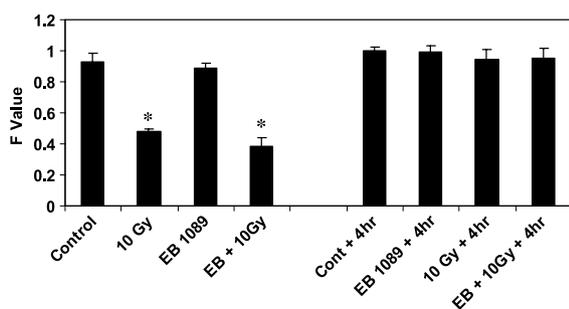irradiation, indicating that the rate of DNA repair (presumptively the repair of double-strand breaks) was unaltered by EB 1089. Again, these data are consistent with the findings relating to the overall repair of DNA damage monitored by alkaline unwinding as shown in Fig. 1.

ROS Generation in Potentiation of the Response to Radiation by EB 1089 in the Breast Tumor Cell

Several studies have implicated the generation of ROS in the enhancement of the response to the antitumor drug, doxorubicin, and tumor necrosis factor by $1,25(OH)_2D_3$ as well as by vitamin D_3 analogues (25, 26). To determine whether EB 1089 might influence reactive oxygen generation in cells exposed to IR, MCF-7 cells were treated with 10 Gy radiation alone or radiation preceded by EB 1089; dichlorofluorescein diacetate was used as a fluorescent probe to measure overall oxidative stress, which would reflect ROS generation in the cells. Figure 3 indicates that minimal ROS was detected after radiation alone; in contrast, when the cells were first treated with EB 1089, a significant degree of ROS was detected 72 hours after irradiation. Figure 3 further shows that GSH blocks the generation of ROS by EB 1089 plus radiation. (It should be emphasized that these experiments are not measuring direct ROS generation by irradiation but ROS that could be the consequence of, for example, delayed DNA damage effects on mitochondrial function).

To determine whether ROS generation might contribute to the radiation-induced cell death promoted by EB 1089, cell viability was determined after either radiation alone or EB 1089 followed by radiation in the presence of GSH. As shown in Fig. 3B, the cell death that occurred in the cells exposed to EB 1089 followed by radiation was not attenuated by the GSH treatment. Similarly, the free radical scavenger, *N*-acetyl-L-cysteine, blocked free radical generation but failed to alter the promotion of cell death in cells treated with EB 1089 before irradiation (data not shown). As a positive control, both GSH and *N*-acetyl-L-cysteine were shown to interfere with the cytotoxicity of H_2O_2 (data not shown).

Influence of Caspase-3 Expression on the Differential Response to Radiation and EB 1089 followed by Radiation in the MCF-7 Breast Tumor Cells

We have reported previously that exposure to the vitamin D_3 analogue EB 1089, before either radiation or Adriamycin, promotes apoptosis in MCF-7 breast tumor cells in culture (2–5); the combination of EB 1089 with radiation also promotes apoptosis in breast tumor xenografts (6). However, apoptotic cell death is unlikely to play a significant role in the response to this sequence of treatment given that the maximal extent of apoptosis observed at any given time point represents no more than 6% of the cell population (5). This low level of apoptosis may relate, in part, to the fact that MCF-7 cells do not express the executioner caspase, caspase-3 (27). Although we have shown previously that EB 1089 potentiates the response to radiation in ZR-75 breast tumor cells that express caspase-3 (3), we deemed it important to assess the nature of the temporal response in MCF-7 cells engineered to express caspase-3.

Figure 1. Assessment of DNA damage and repair by alkaline unwinding. MCF-7 cells were exposed to 10 Gy irradiation with and without EB 1089 (*EB*) pretreatment. Cells were assessed for irradiation-induced DNA fragmentation immediately after irradiation as well as 4 h after irradiation. *Columns,* average of three independent experiments; *bars,* SE. *, significantly different from control, *P* < 0.05.
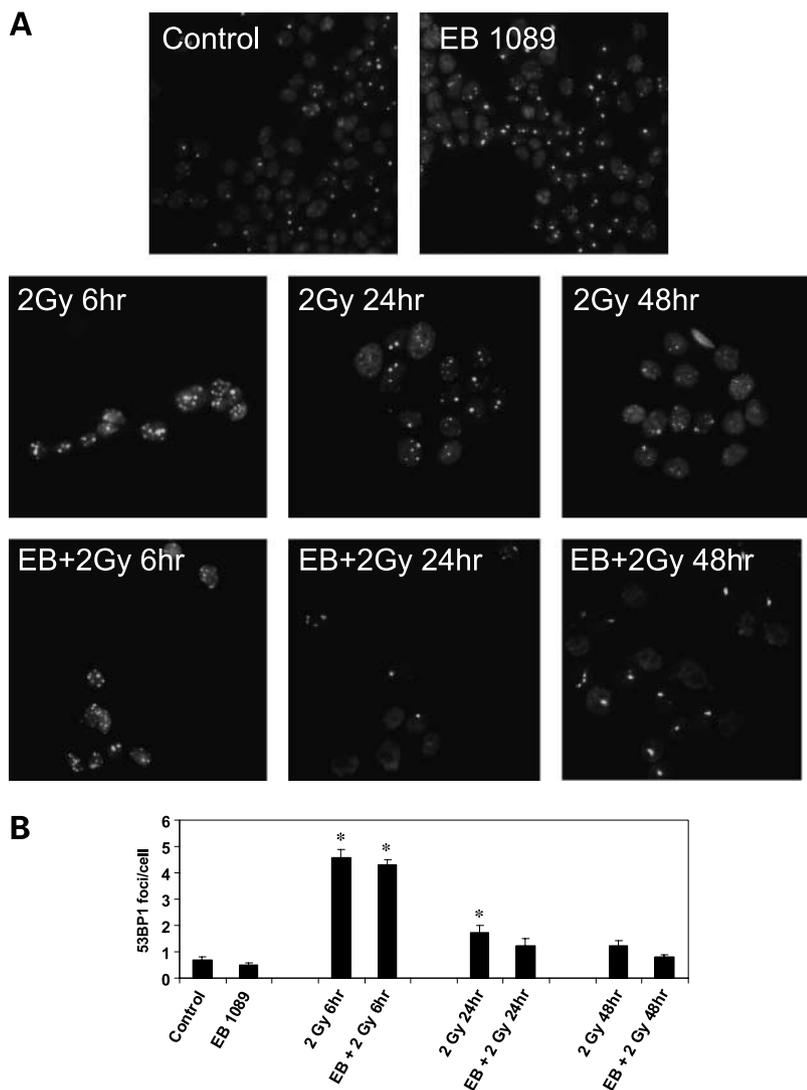
A

B

Figure 2. Assessment of DNA damage and repair by 53BP1 foci formation. MCF-7 cells were exposed to 2 Gy IR with and without pretreatment with EB 1089. At 6, 24, and 48 h after irradiation, cells were fixed and 53BP1 foci were visualized with immunohistochemistry as described in Materials and Methods. **A,** pictures were taken with the blue (488 nmol/L) excitation light. Magnification, ×20. **B,** average number of foci per cell. *Columns,* average of three representative fields per treatment condition; *bars,* SE. *, significantly different from untreated control, $P < 0.05$. Similar results were obtained in a replicate experiment.

Figure 4A shows that the response to radiation alone in MCF-7/caspase-3 cells was quite similar to that observed in the WT MCF-7 cells (5), albeit with increased cell killing by radiation alone. Initially, cell proliferation was only slightly perturbed as the cells continued to divide, albeit at a slightly reduced rate compared with controls (data not shown); subsequently, a significant degree of cell death was detected, with substantial apoptosis evident 3 days after the last radiation dose ($\sim$20% apoptosis based on cell cycle analysis; data not shown). In addition, similar to our observations in WT MCF-7 cells, radiation promoted senescence in the MCF-7/caspase-3 cells (Fig. 4B). Finally, and again as with the WT MCF-7 cells, proliferative recovery was evident between 12 to 15 days after irradiation alone.

Figure 4A indicates that treatment of the cells with EB 1089 before radiation eliminated the early proliferative phase and furthermore resulted in an immediate decline in cell number, similar to our previous observations in WT MCF-7 cells (5). Senescence was detected in the residual cell population (Fig. 4B and C), again consistent with our findings in WT MCF-7 cells (5). It should be noted that no senescent cells were observed in untreated cell cultures or cells treated with EB 1089 alone (data not shown). The extent of radiation-induced apoptosis was slightly increased by EB 1089 at both 24 hours (from 2.7 to 6.4%) and 72 hours (from 21.8 to 27.9%) after radiation (data not shown); more importantly, EB 1089 seemed to entirely eliminate the capacity of the cells to recover proliferative capacity. As a consequence, there was a pronounced reduction in viable cell number under the conditions of EB 1089 preceding irradiation compared with radiation alone.

Response to IR and EB 1089 followed by IR in MCF-7 Cells Lacking p53

In previous studies, we reported that potentiation of the response to IR by EB 1089 is dependent on the cells expressing functional p53 (3, 4); however, the basis for the lack of effect of EB 1089 on sensitivity to radiation in cells that are either mutant or null for p53 was not understood.

To more definitely characterize the nature of the response in cells lacking functional p53, we evaluated the temporal response to both IR and EB 1089 followed by IR in MCF-7/E6 cells with attenuated p53 function. The absence of radiation-induced increases of both p53 and its transactivational target, p21, was confirmed by Western blotting (data not shown).

Figure 5 shows that the MCF-7/E6 cells exposed to radiation alone initially respond similarly to the WT MCF-7 cells and continue to proliferate; however, subsequently, cell death occurs but without evidence for proliferative recovery. In response to EB 1089 followed by radiation, the MCF-7/E6 cells undergo extensive cell death. Consequently, after 7 days, there is no detectable difference in cell number with radiation alone and with EB 1089 preceded by radiation. IR alone promotes apoptosis in MCF-7/E6 cells, but EB 1089 does not increase the extent of radiation-induced apoptosis (data not shown). Taken together with our findings in both the WT MCF-7

A w/o GSH w/ GSH

10 Gy IR

EB 1089 + 10 Gy IR

B

Figure 3. Effects of GSH on the response to EB 1089 plus 10 Gy IR. MCF-7 cells were exposed to 10 Gy IR with or without prior treatment with 100 nmol/L EB 1089 for 72 h. Where indicated, cells were also exposed to GSH (5 mmol/L) for 3 h before irradiation. **A,** ROS generation was determined by dichlorofluorescein diacetate fluorescence. **B,** cell viability was determined at the indicated times after IR. Viability is expressed as a percentage of initial cell number. *Points,* average of two independent experiments; *bars,* range.

and the MCF-7/caspase-3 cells, these studies suggest that the sensitizing effects of EB 1089 on the response to IR seem to be related primarily to interference with the proliferative recovery that is evident in cells expressing functional p53.

The Potential Involvement of c-*myc* in Senescence by Radiation and Cell Death by EB 1089 Plus Radiation

MCF-7 cells treated with IR or the antitumor drug, Adriamycin, undergo a senescent-like growth arrest (5, 13, 28). In previous work, we determined that both Adriamycin and IR suppress the expression of the c-*myc* oncogene (29–31). Furthermore, the extent of c-*myc* suppression was found to correlate quite closely with growth arrest (30, 31). Consequently, it seemed possible that drug- and radiation-induced down-regulation of c-*myc* might promote senescence; furthermore, we postulated that pretreatment with the vitamin D_3 analogue EB 1089 might interfere with the down-regulation of c-*myc*, thereby preventing senescence and promoting cell death (5).

To determine whether c-*myc* might be differentially regulated after treatment with radiation alone versus radiation preceded by EB 1089, MCF-7 cells were treated with 10 Gy IR, 100 nmol/L EB 1089, or 100 nmol/L EB 1089 followed by 10 Gy IR. Figure 6A (*top*) indicates that 10 Gy IR causes suppression of the c-*myc* protein after both 24 and 48 hours, whereas pretreatment with EB 1089 attenuates the capacity of radiation to suppress c-*myc* expression.

The experiments presented in Fig. 6A raised the possibility that maintenance of c-*myc* expression could convert the senescence response to one of cell death. To address this question, studies were designed using MCF-7/35im cells with a doxycycline-inducible myc transgene (15). Figure 6A (*bottom*) shows that 1 μg/mL doxycycline induces c-*myc* in the MCF-7/35im cells and that 10 Gy irradiation fails to suppress the doxycycline-induced myc expression. The resurgence of c-*myc* levels is most pronounced at 72 hours, an effect that has been reproduced in similar studies using Adriamycin.[4]

MCF-7/35im cells were treated with 10 Gy irradiation in the absence or presence of 1 μm/mL doxycycline and cell viability was determined as a function of time by trypan blue exclusion. Figure 6B indicates that the 35im cells, in which c-*myc* levels were maintained with doxycycline, respond to radiation in an essentially identical manner as the MCF-7 cells where c-*myc* was suppressed by irradiation, with an initial period of continued proliferation followed by growth arrest. Figure 6C further indicates that the growth arrest response in the MCF-7/35im cells had characteristics of senescence (β-galactosidase expression, enlarged and flattened cells), both with and without c-*myc* induction.

To determine whether maintenance of c-*myc* levels by EB 1089 interferes with the promotion of radiation-induced cell death, the effects of EB 1089 followed by irradiation were
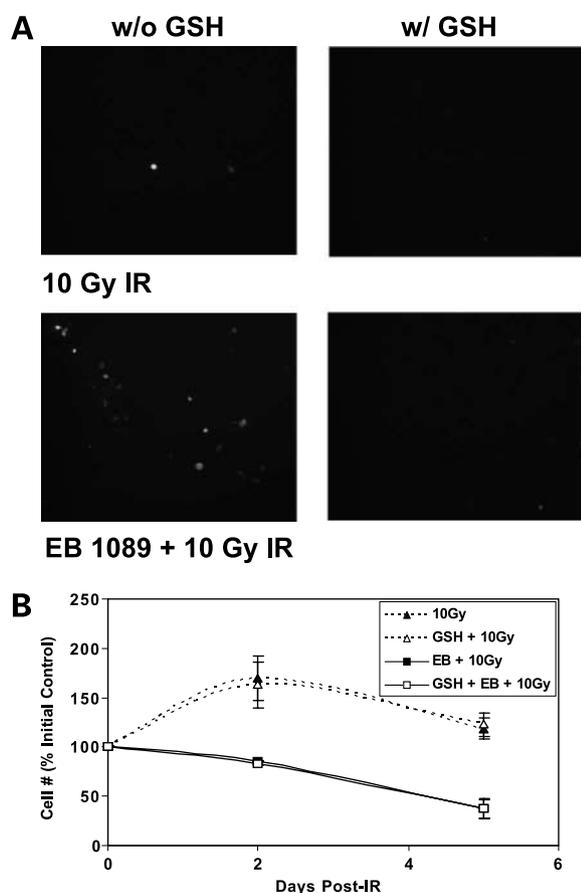
_____

[4] In preparation.

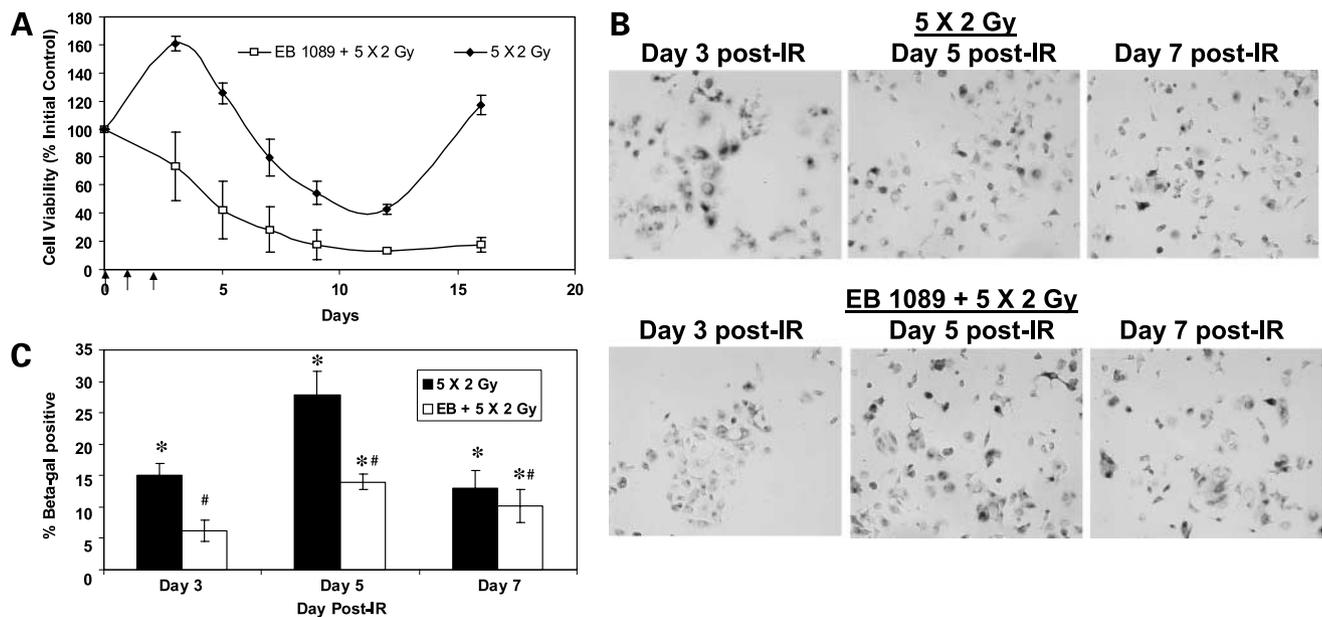Mol Cancer Ther 2006;5(11). November 2006

Figure 4. Influence of EB 1089 on the response to radiation in MCF-7/caspase-3 cells. Cells were exposed to 5 × 2 Gy IR or EB 1089 followed by 5 × 2 Gy IR. **A,** viable cell number was determined by exclusion of trypan blue at the indicated days following the initiation of radiation exposure. *Arrows,* days on which cell irradiation was done. *Points,* average of three experiments; *bars,* SE. **B,** at the indicated times after IR, cells were assessed for β-galactosidase expression as described in Materials and Methods. Pictures taken with inverted microscope at ×20. **C,** percentage of β-galactosidase-positive cells. *Columns,* average of four representative fields taken from two independent experiments; *bars,* SE. *, significantly different from untreated control, $P < 0.05$; #, combination treatment is significantly different from radiation alone, $P < 0.05$.

evaluated in the c-*myc*-inducible cells. Figure 6B shows that the temporal response to EB 1089 plus irradiation was identical with and without induction of c-*myc* by doxycycline. Taken together, these studies seem to rule out a central role for c-*myc* in either the senescence response to radiation or the cell death response in cells exposed to EB 1089 before irradiation.

Assessment of Mitotic Catastrophe in Response to Radiation Alone and EB 1089 Plus Radiation

Our previous studies suggested that apoptosis is likely to play only a small role in the cell death response to EB 1089 plus radiation (5). Other forms of cell death are known to occur after both EB 1089 and radiation treatment, including mitotic catastrophe (32) as well as autophagy (33, 34). To characterize this nonapoptotic cell death, the role of mitotic catastrophe and autophagy were assessed after EB 1089 plus radiation treatment.

Mitotic catastrophe is characterized by the formation of micronuclei (32). These can be visualized as decondensed chromatin in small micronuclei lying outside of the main nucleus in cells that have attempted but failed to divide. To determine the role of mitotic catastrophe in the response to fractionated radiation as well as whether EB 1089 may increase radiation-induced mitotic catastrophe, MCF-7 cells were grown on glass coverslips and exposed to 5 × 2 Gy IR with and without prior exposure to 100 nmol/L EB 1089 for 72 hours. At 1, 3, 5, and 7 days after irradiation, cells were stained with DAPI to visualize their nuclear content and micrographs were taken using a laser scanning microscope. As shown in the representative experiment presented in

Fig. 8A, micronuclei were observed in cells treated with 5 × 2 Gy as well as EB 1089 plus 5 × 2 Gy. There are clearly small micronuclei lying outside of the main nuclei in these binucleated cells, which are not visible in the micrographs taken of untreated control cells (Fig. 7A) or when cells were exposed to EB 1089 alone (data not shown). The micronuclei were scored as described in Materials and Methods, and the percentage of micronucleated binucleated cells is presented in Fig. 7B. One day after exposure to radiation, ~75% of the binucleated cells contain micronuclei. This suggests that the cells that have attempted to undergo mitosis at this time have subsequently undergone mitotic
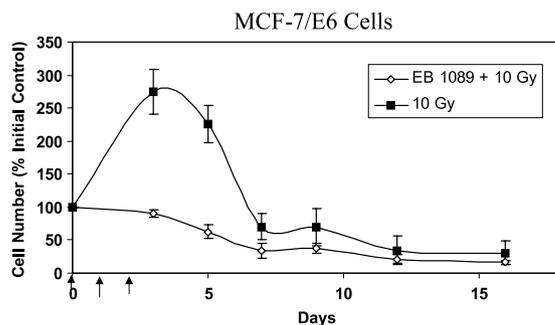

Figure 5. The influence of EB 1089 on the temporal response to fractionated radiation in MCF-7/E6 cells. Viable cell number was determined by exclusion of trypan blue at indicated days following the initiation of radiation exposure. *Arrows,* days on which irradiation was done. *Points,* average of two to four experiments; *bars,* SE.
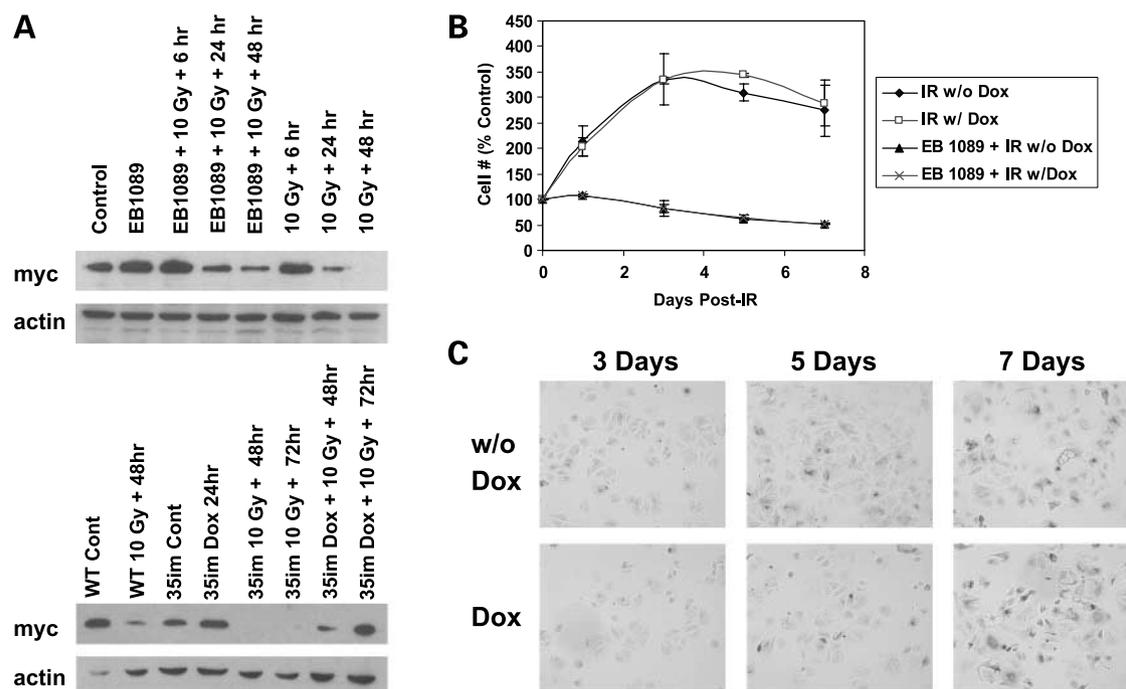
Figure 6. Effects of EB 1089 and 10 Gy on the expression of myc in MCF-7 cells. **A,** MCF-7/WT and MCF-7/35im cells were treated with 10 Gy IR and the expression of myc was assessed by Western blotting at the indicated time points after irradiation. Where indicated, the MCF-7/35im cells were also coincubated with 1 μg/mL doxycycline (*Dox*). The expression of actin was used as a loading control. **B,** cell viability was determined at the indicated time points following irradiation by trypan blue exclusion. *Points,* average of two independent experiments; *bars,* range. **C,** at the indicated times after irradiation, cells were assessed for β-galactosidase expression as described in Materials and Methods. Pictures were taken with an inverted microscope at ×20.

catastrophe. The percentage declines to below 50% by day 7 after irradiation, as more cells are able to successfully complete mitosis. EB 1089 does not seem to alter the response to radiation in terms of the induction of mitotic catastrophe. The percentage of micronucleated binucleated cells for the combination of EB 1089 plus radiation (open squares) is essentially the same as for radiation alone (Fig. 7B).

Although a high percentage of the cells that continue through mitosis subsequently undergo mitotic catastrophe after either radiation or EB 1089 plus radiation, the percentage of mitotic cells (as measured by the percentage of binucleated cells, closed triangles) never exceeds 20% of the total cell population. This indicates that the percentage of cells that undergo mitotic catastrophe is a small fraction of the overall cell population. These data further suggest that mitotic catastrophe likely plays a relatively limited role in the overall cell death response following either fractionated irradiation alone or the combination of EB 1089 plus radiation.

EB 1089 Increases Radiation-Induced Autophagy

To determine whether autophagy might contribute to the effects of EB 1089 on the response to IR (22, 33), cells were treated with EB 1089, 5 × 2 Gy IR, or the combination of EB 1089 followed by 5 × 2 Gy IR, and the lysosomotropic agent acridine orange was used as a marker for detecting the acidic compartments of the cells. When acridine orange encounters an acidic environment, such as a lysosome or autophagosomes, its fluorescence changes from green to red (22, 35). As shown in Fig. 8, vital staining of MCF-7 cells with acridine orange revealed the appearance of acidic vesicular organelles after exposure to both 5 × 2 Gy and EB 1089 followed by 5 × 2 Gy IR. The 4-day exposure to 2.5 μmol/L tamoxifen was used as a positive control, as this agent has been shown previously to induce autophagy in MCF-7 cells (33). Dye in the acidic vesicular organelle fluoresces bright red, whereas the nucleus and cytoplasm stain predominantly green. Fig. 8A and B indicates that the increase in acidic vesicular organelles occurred earlier and to a much greater extent in irradiated cells pretreated with EB 1089 compared with cells treated with radiation alone. Over 50% of the cells treated with the combination of EB 1089 plus radiation had increases in acidic vesicular organelles, similar to that detected with exposure to tamoxifen. Untreated control cells as well as cells treated with EB 1089 alone show minimal red fluorescence. These data indicate that EB 1089 increases radiation-induced autophagy.

Discussion

DNA Damage and Repair

The current studies using alkaline unwinding and 53BP1 foci formation support the conclusion that EB 1089 fails to increase the extent of DNA damage induced by radiation.

The current work also indicates that EB 1089 does not interfere with DNA repair. Taken together, these studies strongly suggest that the cell death induced by radiation under conditions where radiation is preceded by exposure to EB 1089 is likely to be a consequence of alterations in cell signaling pathways downstream of the initial induction of DNA damage.

Generation of Free Radicals

In view of several reports indicating a role for reactive oxygen in potentiation of the response to antitumor compounds, such as doxorubicin (25) and tumor necrosis factor (26) by vitamin D₃ and its analogues, we evaluated both the generation of ROS by EB 1089 and radiation as well as the effect of free radical scavengers on the tumor cell response to treatment. We clearly detected ROS generation in cells exposed to EB 1089 before irradiation. It should be emphasized that this is not ROS generation associated with the initial damage to DNA but subsequent and delayed ROS that is presumably related to mitochondrial dysfunction (36). This suggests that ROS are not a direct consequence of radiation interaction with the tumor cell but are likely to be part of a signaling response pathway. The free radical scavengers, *N*-acetyl-L-cysteine and GSH, blocked the generation of reactive oxygen but failed to alter the temporal response after EB 1089 followed by radiation. Based on the lack of protection by free radical scavengers as well as the relatively low level of ROS generation, we conclude that the enhanced response to radiation that is promoted by EB 1089 is unlikely to be a consequence of increased reactive oxygen.

Senescence and Apoptosis

We have reported recently that IR (both a single dose of 10 Gy as well as a cumulative dose of 10 Gy from fractionated doses of 2 Gy) promotes an accelerated senescence response in MCF-7 breast tumor cells (5, 13). One possible explanation for this observation is that senescence is a default response in cells that are refractory to apoptosis as a consequence of the lack of caspase-3. However, we as well as others have reported accelerated senescence in response to chemotherapy and radiation in cells expressing functional caspase-3 (37, 38). Furthermore, our current work indicates that senescence is the primary response to radiation alone even in cells expressing caspase-3.

The MCF-7/caspase-3 cells also have a similar response to EB 1089 plus radiation as the parental MCF-7 cells, that of cell death. Again, as with parental MCF-7 cells, senescence is evident in the residual surviving cell population. Perhaps of greatest interest is the fact that EB 1089 essentially obliterates the proliferative recovery observed in cells exposed to radiation alone. This suggests that the effect of EB 1089 treatment on the radiation response is also likely to be evident in cells that are highly "apoptotic competent," such as the MCF-7 cells expressing functional caspase-3.

c-*myc*

c-*myc* is an oncogene that is critically important for several signal transduction pathways involved in differentiation, growth arrest, and cell death (39). Under physiologic conditions, c-*myc* may promote cellular replication by activating positive regulators of cell division, such as cyclin D1 and D2, as well as cyclin-dependent kinase 4 and E2F2 (40). c-*myc* may also suppress growth-inhibitory genes, such as the cyclin-dependent kinase inhibitors p21, p27, and p19 (41).

c-*myc* also seems to be an important component of the signal transduction pathways responsible for the DNA damage response. c-*myc* has been implicated in the cell cycle arrest resulting from exposure to agents that cause DNA damage, such as UV and IR as well as Adriamycin (42). Previous studies from our laboratory have shown that
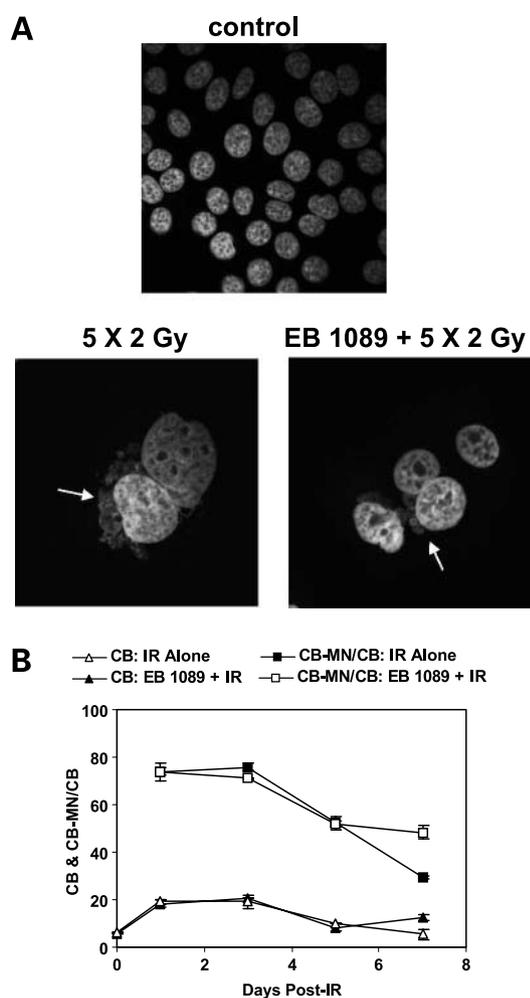

Figure 7. Detection of micronuclei in MCF-7 cells treated with radiation alone and radiation preceded by EB 1089. MCF-7 cells were treated with 100 nmol/L EB 1089, 5 × 2 Gy IR, or EB 1089 followed by 5 × 2 Gy IR. Micronuclei formation was assessed by DAPI staining. **A,** pictures were taken using a Zeiss laser scanning microscope. *Arrows,* micronuclei. Magnifications, ×40 (control) and ×100 (IR and EB 1089 + IR). **B,** at the indicated days after irradiation, the percentage of binucleated cells (*CB*) and the percentage of binucleated cells with micronuclei (*CB-MN/CB*) were determined as described in Materials and Methods. *Points,* average of two independent experiments; *bars,* range.

Figure 8. Detection of acidic vesicular organelles (*AVO*) by vital staining with acridine orange in MCF-7 breast tumor cells. MCF-7 cells were treated with 100 nmol/L EB 1089, 5 × 2 Gy IR, or EB 1089 followed by 5 × 2 Gy IR. The induction of acidic vesicular organelle was assessed at the indicated days after irradiation by staining for 15 min with 1 μg/mL acridine orange. **A,** pictures were taken using a fluorescent microscope with a magnification of ×20. **B,** the percentage of cells with increased acidic vesicular organelle were counted at the indicated days after irradiation. *Columns,* average of at least four representative fields per treatment condition; *bars,* SE. Similar results were obtained a replicate experiment.
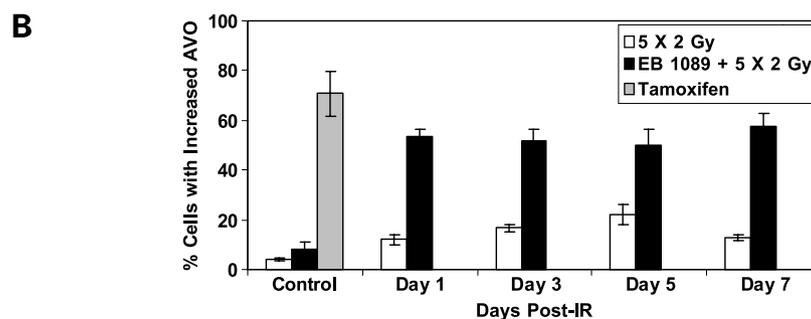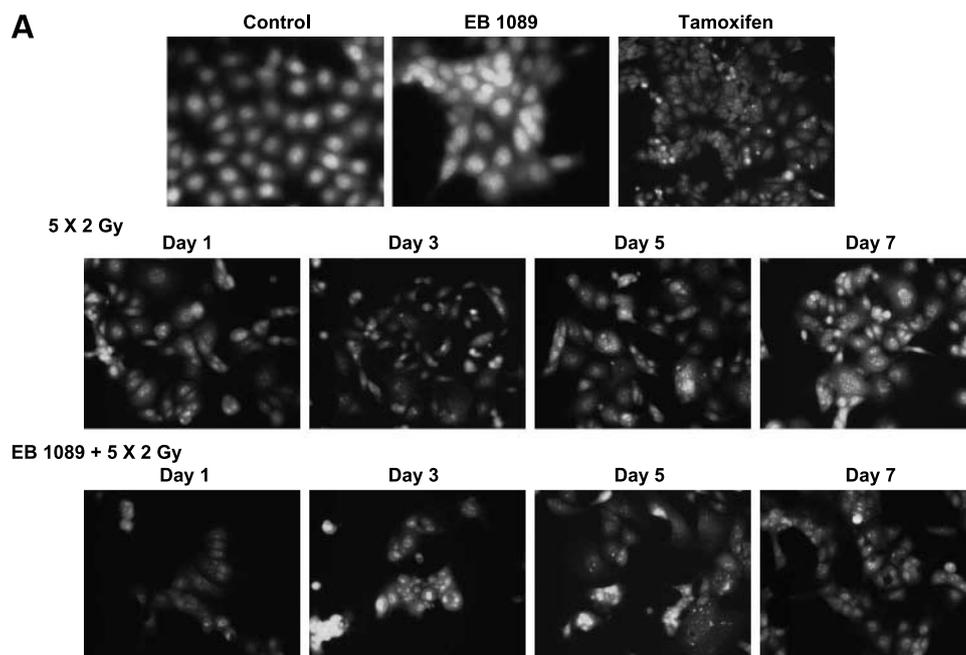
suppression of myc expression in MCF-7 breast tumor cells correlates closely with the extent of growth arrest induced by either Adriamycin or IR (30, 31). Suppression of c-*myc* has also been linked to down-regulation of hTERT, the catalytic subunit of telomerase, the enzyme that extends the telomere and thereby prevents the induction of senescence (43). In contrast, maintenance or overexpression of c-*myc* has been associated with the promotion of apoptotic cell death (44).

We found that whereas c-*myc* protein levels were suppressed by radiation alone, c-*myc* levels were sustained with prior exposure to EB 1089. This raised the intriguing possibility that maintenance of c-*myc* expression by EB 1089 might be responsible for the promotion of cell death, possibly through apoptosis, whereas suppression of c-*myc* could be linked to senescence. However, this does not seem to be the case. When MCF-7 cells with doxycycline-inducible c-*myc* were exposed to radiation, an identical senescence response was noted as in parental MCF-7 cells. Furthermore, when these cells were exposed to EB 1089 before radiation, we noted cell death and interference with proliferative recovery. An identical senescence response was observed following Adriamycin treatment in MCF-7 cells with and without doxycycline as well.[4] Consequently, c-*myc* does not appear to play a central role in either senescence or cell death in irradiated breast tumor cells.

Autophagic Cell Death and Proliferative Recovery

Our findings relating to the promotion of autophagic cell death in irradiated cells with prior exposure to EB 1089 lead to several tentative conclusions and open the way for additional experiments to elucidate the signaling pathways involved in potentiation of radiation sensitivity. It seems possible that the capacity of EB 1089 to confer sensitivity to radiation is primarily a function of the promotion of autophagy. Consequently, it is likely that EB 1089 may influence signaling molecules associated with regulation of autophagic cell death. Furthermore, there is evidence that autophagy may be dependent on functional p53 (45), which might further explain the lack of sensitization in p53-mutant or p53-null breast tumor cells.

It is also necessary to consider the effects of EB 1089 on proliferative recovery. In our hands, we observe proliferative recovery only in cells that express functional p53

(13, 46). This is not a uniform observation, as others have reported recovery or escape from senescence in p53-null lung cancer cells (47). At this juncture, we do not fully understand the lack of recovery in the cells without functional p53, although this may relate to the ability of these cells to undergo apoptosis. However, as both MCF-7/E6 and MCF-7/caspase-3 cells die in part by apoptosis, this again argues in support of the idea that recovery might be related to the presence of p53.

Potential Clinical Ramifications

In general, the conventional therapies of breast cancer that involve surgery, radiation, and/or chemotherapy are quite effective in elimination of the primary tumor, particularly in the context of early detection. Unfortunately, although many patients are cured, there is a subset of patients that experience morbidity and mortality as a consequence of disease recurrence or metastatic spread of the disease, often to the brain or bone. The potential clinical significance of the current studies lies in the possibility that the inclusion of vitamin D₃ or vitamin D₃ analogues in association with radiotherapy and chemotherapy may promote cell death through alternative pathways, such as autophagy and thereby prevent (or at least attenuate and delay) the proliferative recovery that could contribute to disease recurrence. In terms of the potential selectivity involved in the use of vitamin D₃ or its analogues, previous work from this laboratory has shown the radiosensitizing effects of vitamin D₃ analogues to be selective for the tumor cell, as radiation sensitivity was not altered in normal breast epithelial cells or BJ fibroblasts (5, 48).

References

1. Hansen CM, Binderup L, Hamberg KJ, Carlberg C. Vitamin D and cancer: effects of 1,25(OH)2D3 and its analogs on growth control and tumorigenesis. Front Biosci 2001;6:D820–48.

2. Sundaram S, Chaudhry M, Reardon D, Gupta M, Gewirtz DA. The vitamin D3 analog EB 1089 enhances the antiproliferative and apoptotic effects of Adriamycin in MCF-7 breast tumor cells. Breast Cancer Res Treat 2000;63:1–10.

3. Sundaram S, Gewirtz DA. The vitamin D3 analog EB 1089 enhances the response of human breast tumor cells to radiation. Radiat Res 1999; 152:479–86.

4. Chaudhry M, Sundaram S, Gennings C, Carter H, Gewirtz DA. The vitamin D3 analog, ILX-23-7553, enhances the response to Adriamycin and irradiation in MCF-7 breast tumor cells. Cancer Chemother Pharmacol 2001;47:429–36.

5. DeMasters GA, Gupta MS, Jones JR, et al. Potentiation of cell killing by fractionated radiation and suppression of proliferative recovery in MCF-7 breast tumor cells by the Vitamin D3 analog EB 1089. J Steroid Biochem Mol Biol 2004;92:365–74.

6. Sundaram S, Sea A, Feldman S, et al. The combination of a potent vitamin D3 analog, EB 1089, with ionizing radiation reduces tumor growth and induces apoptosis of MCF-7 breast tumor xenografts in nude mice. Clin Cancer Res 2003;9:2350–6.

7. Light BW, Yu WD, McElwain MC, Russell DM, Trump DL, Johnson chondroitin sulfate. Potentiation of cisplatin antitumor activity using a vitamin D analogue in a murine squamous cell carcinoma model system. Cancer Res 1997;57:3759–64.

8. Hershberger PA, Yu WD, Modzelewski RA, Rueger RM, Johnson chondroitin sulfate, Trump DL. Calcitriol (1,25-dihydroxycholecalciferol) enhances paclitaxel antitumor activity *in vitro* and *in vivo* and accelerates paclitaxel-induced apoptosis. Clin Cancer Res 2001;7:1043–51.

9. Ahmed S, Johnson CS, Rueger RM, Trump DL. Calcitriol (1,25-dihydroxycholecalciferol) potentiates activity of mitoxantrone/dexamethasone in an androgen independent prostate cancer model. J Urol 2002; 168:756–61.

10. Tanaka H, Yamamuro T, Kotoura Y, et al. 1 α,25(OH)2D3 exerts cytostatic effects on murine osteosarcoma cells and enhances the cytocidal effects of anticancer drugs. Clin Orthop Relat Res 1989;247: 290–6.

11. Vink-van Wijngaarden T, Pols HA, Buurman CJ, et al. Inhibition of breast cancer cell growth by combined treatment with vitamin D3 analogues and tamoxifen. Cancer Res 1994;54:5711–7.

12. Nolan E, Donepudi M, VanWeelden K, Flanagan L, Welsh J. Dissociation of vitamin D3 and anti-estrogen mediated growth regulation in MCF-7 breast cancer cells. Mol Cell Biochem 1998;188:13–20.

13. Jones KR, Elmore LW, Jackson-Cook C, et al. p53-Dependent accelerated senescence induced by ionizing radiation in breast tumor cells. Int J Radiat Biol 2005;81:445–58.

14. Ylikomi T, Laaksi I, Lou YR, et al. Antiproliferative action of vitamin D. Vitam Horm 2002;64:357–406.

15. Venditti M, Iwasiow B, Orr FW, Shiu RP. C-*myc* gene expression alone is sufficient to confer resistance to antiestrogen in human breast cancer cells. Int J Cancer 2002;99:35–42.

16. Wang Q, Yang W, Uytingco MS, Christakos S, Wieder R. 1,25-dihydroxyvitamin D3 and all-*trans*-retinoic acid sensitize breast cancer cells to chemotherapy-induced cell death. Cancer Res 2000;60:2040–8.

17. Gavrielli Y, Sherman Y, Ben-Sasson SA. Identification of programmed cell death *in situ* via specific labeling of nuclear DNA fragmentation. J Cell Biol 1992;119:493–501.

18. Kantor PM, Schwartz HS. A fluorescence enhancement assay for cellular DNA damage. Mol Pharmacol 1982;22:145–51.

19. Dimri GP, Lee X, Basile G, et al. A biomarker that identifies senescent human cells in culture and in aging skin *in vivo*. Proc Natl Acad Sci U S A 1995;92:9363–7.

20. Mochan TA, Venere M, DiTullio RA Jr, Halazonetis TD. 53BP1, an activator of ATM in response to DNA damage. DNA Repair (Amst) 2004;3: 945–52.

21. Song YS, Lee BY, Hwang ES. Dinstinct ROS and biochemical profiles in cells undergoing DNA damage-induced senescence and apoptosis. Mech Ageing Dev 2005;126:580–90.

22. Paglin S, Hollister T, Delohery T, et al. A novel response of cancer cells to radiation involves autophagy and formation of acidic vesicles. Cancer Res 2001;61:439–44.

23. Paglin S, Delohery T, Erlandson R, Yahalom J. Radiation-induced micronuclei formation in human breast cancer cells: dependence on serum and cell cycle distribution. Biochem Biophys Res Commun 1997;237: 678–84.

24. Jackson SP. Sensing and repairing DNA double-strand breaks. Carcinogenesis 2002;23:687–96.

25. Ravid A, Rocker D, Machlenkin A, et al. 1,25-Dihydroxyvitamin D3 enhances the susceptibility of breast cancer cells to doxorubicin-induced oxidative damage. Cancer Res 1999;59:862–7.

26. Weitsman GE, Ravid A, Ligerman UA, Koren R. Vitamin D enhances caspase-dependent and -independent TNF-α-induced breast cancer cell death: The role of reactive oxygen species and mitochondria. Int J Cancer 2003;106:178–86.

27. Kurokawa H, Nishio K, Fukumoto H, Tomonari A, Suzuki T, Saijo N. Alteration of caspase-3 (CPP32/Yama/apopain) in wild-type MCF-7, breast cancer cells. Oncol Rep 1999;6:33–7.

28. Elmore LW, Rehder CW, Di X, et al. Adriamycin-induced senescence in breast tumor cells involves functional p53 and telomere dysfunction. J Biol Chem 2002;277:35509–15.

29. Fornari FA, Jr., Jarvis WD, Grant S, et al. Induction of differentiation and growth arrest associated with nascent (nonoligosomal): DNA fragmentation and reduced c-*myc* expression in MCF-7 human breast tumor cells after continuous exposure to a sublethal concentration of doxorubicin. Cell Growth Differ 1994;5:723–33.

30. Fornari FA, Jr., Jarvis DW, Grant S, et al. Growth arrest and non-apoptotic cell death associated with the suppression of c-*myc* expression in MCF-7 breast tumor cells following acute exposure to doxorubicin. Biochem Pharmacol 1996;51:931–40.

31. Watson NC, Di YM, Orr MS, et al. Influence of ionizing radiation on

proliferation, c-*myc* expression and the induction of apoptotic cell death in two breast tumour cell lines differing in p53 status. Int J Radiat Biol 1997; 72:547 – 59.

32. Roninson IB, Broude EV, Chang BD. If not apoptosis, then what? Treatment-induced senescence and mitotic catastrophe in tumor cells. Drug Resist Updat 2001;4:303 – 13.

33. Hoyer-Hansen M, Bastholm L, Mathiasen IS, Elling F, Jaattela M. Vitamin D analog EB1089 triggers dramatic lysosomal changes and Beclin 1-mediated autophagic cell death. Cell Death Differ 2005;12:1297 – 309.

34. Mains RE, May V. The role of a low pH intracellular compartment in the processing, storage, and secretion of adrenocorticorticotropic hormone and endorphin. J Biol Chem 1988;263:7887 – 94.

35. Traganos F, Darzynkiewicz Z. Lysosomal proton pump activity: supravital cell staining with acridine orange differentiates leukocyte subpopulations. Methods Cell Biol 1994;41:185 – 94.

36. Cai J, Jones DP. Superoxide in apoptosis. Mitochondrial generation triggered by cytochrome *c* loss. J Biol Chem 1998;273:11401 – 4.

37. Hattangadi DK, DeMasters GA, Walker TD, et al. Influence of p53 and caspase 3 activity on cell death and senescence in response to methotrexate in the breast tumor cell. Biochem Pharmacol 2004;68: 1699 – 708.

38. Cukusic A, Ivankovic M, Skrobot N, et al. Spontaneous senescence in the MDA-MB-231 cell line. Cell Prolif 2006;39:205 – 16.

39. Liao DJ, Dickson RB. c-Myc in breast cancer. Endocr Relat Cancer 2000;7:143 – 64.

40. Dang CV. c-Myc target genes involved in cell growth, apoptosis, and metabolism. Mol Cell Biol 1999;19:1 – 11.

41. Coller HA, Grandori C, Tamayo P, et al. Expression analysis with oligonucleotide microarrays reveals that MYC regulates genes involved in growth, cell cycle, signaling, and adhesion. Proc Natl Acad Sci U S A 2000;97:3260 – 5.

42. Gewirtz DA. Growth arrest and cell death in the breast tumor cell in response to ionizing radiation and chemotherapeutic agents which induce DNA damage. Breast Cancer Res Treat 2000;62:223 – 35.

43. Wu KJ, Grandori C, Amacker M, et al. Direct activation of TERT transcription by c-MYC. Nat Genet 1999;21:220 – 4.

44. Prendergast GC. Mechanisms of apoptosis by c-Myc. Oncogene 1999;18:2967 – 87.

45. Crighton D, Wilkinson S, O'Prey J, et al. DRAM, a p53-induced modulator of autophagy, is critical for apoptosis. Cell 2006;126:121 – 34.

46. Elmore LW, Di X, Dumur C, Holt SE, Gewirtz DA. Evasion of a single-step, chemotherapy-induced senescence in breast cancer cells: implications for treatment response. Clin Cancer Res 2005;11:2637 – 43.

47. Roberson RS, Kussick SJ, Vallieres E, Chen SY, Wu DY. Escape from therapy-induced accelerated cellular senescence in p53-null lung cancer cells and in human lung cancers. Cancer Res 2005;65:2795 – 803.

48. Polar MK, Gennings C, Park M, Gupta MS, Gewirtz DA. Effect of the vitamin D3 analog ILX 23-7553 on apoptosis and sensitivity to fractionated radiation in breast tumor cells and normal human fibroblasts. Cancer Chemother Pharmacol 2003;51:415 – 21.

Potentiation of radiation sensitivity in breast tumor cells by the vitamin D $_3$ analogue, EB 1089, through promotion of autophagy and interference with proliferative recovery

Gerald DeMasters, Xu Di, Irene Newsham, et al.

Updated version	Access the most recent version of this article at: http://mct.aacrjournals.org/content/5/11/2786

Cited articles	This article cites 46 articles, 18 of which you can access for free at: http://mct.aacrjournals.org/content/5/11/2786.full#ref-list-1
Citing articles	This article has been cited by 6 HighWire-hosted articles. Access the articles at: http://mct.aacrjournals.org/content/5/11/2786.full#related-urls

E-mail alerts	Sign up to receive free email-alerts related to this article or journal.
Reprints and Subscriptions	To order reprints of this article or to subscribe to the journal, contact the AACR Publications Department at pubs@aacr.org.
Permissions	To request permission to re-use all or part of this article, use this link http://mct.aacrjournals.org/content/5/11/2786. Click on "Request Permissions" which will take you to the Copyright Clearance Center's (CCC) Rightslink site.